

Engineering Notes

ENGINEERING NOTES are short manuscripts describing new developments or important results of a preliminary nature. These Notes cannot exceed 6 manuscript pages and 3 figures; a page of text may be substituted for a figure and vice versa. After informal review by the editors, they may be published within a few months of the date of receipt. Style requirements are the same as for regular contributions (see inside back cover).

Manufacturing of Small Rocket Motors

ARTHUR B. CLAYTON*

Lockheed Propulsion Company, Redlands, Calif.

THIS Note discusses fabrication of 3- to 6-in.-diam penetration-aid motors. These motors comprise an integral assembly of an axial-thrust unit and a spin imparting (tangential-thrust) unit. Several impulse levels are provided by replacing part of the propellant with an inert material, keeping unit weight the same.

Operation of the small, multipulse, constant-weight, two-stage rocket motor is initiated by a redundant ignition system consisting of a squib, boosters, SCID's (small column insulated delay), and igniters. The first stage unlatches the motor from its launcher, provides spin stabilization, and provides thrust to propel the payload away from its dispenser. After a prescribed delay period, the second stage imparts an added axial velocity increment. An electrically initiated squib ignites a 300-mg transition booster charge, which ignites four SCID lines. Two of them lead directly to the spin motor igniters; two go to the SCID delay and the main motor pyrogen (igniter). Prior to motor ignition, the Fiberglass-covered SCID line explodes beneath a metal retainer at a predetermined location, resulting in the release of the motor latching mechanism. Then the SCID line ignites the spin motor. This firing action occurs in nominal time of 5 msec. The spin motor imparts a spin rotation to the payload and provides the axial force necessary to eject the payload. This combined motion is achieved by three canted nozzles (Fig. 1). The spin motor achieves peak thrust in approximately 2 to 3 msec in a total burn time of 55 msec, with burning completed prior to leaving the launch tube. In the meantime, the two ignited main motor SCID lines have ignited the in-line, 2-sec ignition delays located in the nozzle of the main motor.

A SCID unit is about the size of a large "strike anywhere" match and consists basically of a piece of slow-burning SCID mounted in a sealed aluminum cylinder. On completion of the slow SCID burning, another piece of fast SCID is ignited and in turn ignites the pyrogen or main motor igniter. Depending on the amount of propellant contained in the main motor, burning times can be varied from 2 to 5 sec with a motor total impulse variation of 73 to 635 sec.

Manufacturing and Assembly of Subsystems, Including Final Assembly of Total System

The small two-stage rocket motor is made up of three major subsystems: spin motor, main motor, and igniter system (pyrogen) (Fig. 2.) The major parts of the spin motor assembly are the chamber (which doubles as main motor aft closure), closure, nozzles, nozzle plugs, propellant, roll pins, main motor nozzle, adhesives, aft closure insulation, and O-rings. Major steps to produce the spin motor included propellant grain fabrication, aft closure assembly, spin motor

closure assembly, propellant loading, and total subsystem assembly.

The first step in propellant preparation is grinding the oxidizer to a particle size to meet the preselected properties. After the grind has been completed and tested for particle size by the Quality Control Laboratory, a portion of the ground oxidizer is used to make a 5000-g laboratory mix. This mix is used to qualify the materials which will be used in the full-scale mix and to set the ratio of ground-to-unground oxidizer in the full-scale mix, thereby providing an additional method for controlling burning rate within specified limits. Fuel slurry materials are then weighed and mixed together into a slurry using a Cowles dissolver. At the end of the mix cycle, a sample of uncured propellant is removed from the mixer and tested. The propellant is then vacuum cast into treated paper containers of sufficient size to fabricate spin-motor grains. After casting, the propellant cartons are placed in cure at $145 \pm 5^\circ\text{F}$ for 120 (+12 or -0) hr. The cured propellant is then tested for density and uniaxial tensile properties.

Packaging of propellants containing alkylferrocene requires special attention to minimize ferrocene migration during the storage period. The propellant-loaded carton is wrapped with aluminum foil and sealed with aluminum tape. The package is overwrapped with conductive polyethylene, including desiccant between the foil and overwrap, after which the overwrap is sealed.

A remote-operated meat slicer is used for rough-cutting the propellant slabs, which are then positioned on a vacuum bed and milled to required thickness dimensions and surface finish. Propellant grains are cut from the slabs by a tool designed on the cookie cutter concept and are arranged in sets and weighed. Grain sets falling within weight tolerances are packaged by the same method as described for ferrocene-type propellants.

The aft closure (spin-motor chamber) subassembly is processed as follows. It is degreased, masked, and all bonding surfaces are wet honed. Immediately before adhesive application, metal surfaces are acid etched, washed, and dried. The bonding surface of the phenolic exit cone is rough-ground using emery cloth, coated with adhesive (PR-1221), pressed into position in the aft closure, and held with a bonding fixture during the cure cycle. During the cure cycle, the aft closure insulation (Buna-N rubber) is prepared for bonding by cleaning with solvent, wet-honing the bonding surface, washing with a detergent, and drying. Adhesive (EPON 934) is applied to both bonding surfaces, aft closure, and insulation. The parts are installed with a bond fixture, with pressure applied over the entire bond line during the cure cycle. Next, the nozzle throat and exit cone are machined. Thrust alignment is maintained by a centering land in the aft closure, which interfaces with a matching land in the main motor thrust chamber.

The spin motor closure assembly is processed by degreasing the metal parts (aluminum spin motor closure and cadmium plated steel nozzles), application of adhesive (EPON 934) to both bonding surfaces, mating, and curing. The engineering design includes a shoulder in the spin motor closure for the nozzle to bear on, so that the adhesive acts primarily as a sealant and secondarily as an adhesive.

Before bonding the propellant to the aft closure and spin-motor closure, both units are wet-honed, acid-etched, and

Presented as Paper 69-520 at the AIAA 5th Propulsion Joint Specialist Conference, U.S. Air Force Academy, Colo., June 9-13, 1969; submitted June 17, 1969; revision received September 17, 1969.

* Senior Manufacturing Engineering.

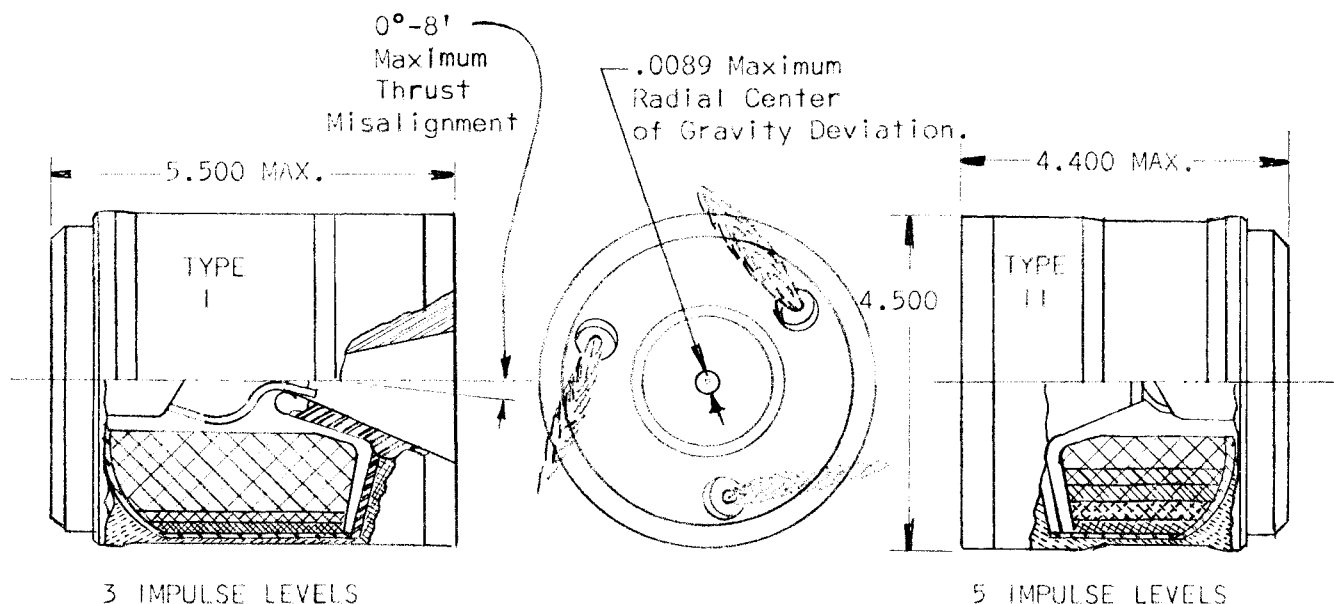


Fig. 1 Sketches of 3- and 5-impulse level motors.

dried. Then a matched set of propellant grains are mated as a unit and controlled as a unit until actual assembly of unit has been completed; adhesive (EPON 934) is applied to the mating surfaces of these grains for the aft closure and the spin-motor closure, and they are held in position on their respective parts with pressure applied by a bonding fixture over the bonding surfaces. The assemblies are then placed into the cure oven at 145° for 120 hr.

On completion of cure, the assemblies are removed from the cure oven, cooled at ambient temperature, and then removed from the bond fixtures, and O-rings are lubricated and placed in the O-ring groove. Scribe marks are utilized to align the spin motor closure to the aft closure with respect to rotational position. The loaded spin-motor closure assembly is pressed down into place, securing the assembly and thus completing the spin motor subassembly, which is then pressure-checked for O-ring integrity.

The second major subassembly, the main motor thrust chamber, is assembled from the chamber, insulation, inert filler (where applicable), liner, adhesive, and propellant.

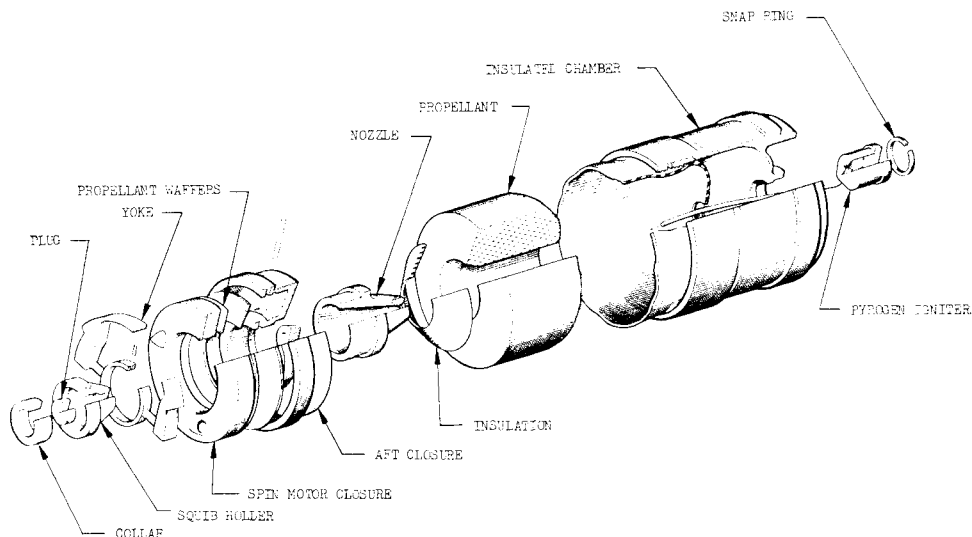
The next subassembly, the igniter (or pyrogen) is processed at the same time as the spin motor and the main motor, so that all three will progress into final assembly together. The pyrogen igniter is composed of plug, propellant grain,

Pyro-Pak, SCID, chamber, adhesives, and O-rings. The igniter grain is fabricated in the same manner as the spin motor propellant grain. The pyrogen grains are then bonded to the pyrogen phenolic plug. The edge of grain is inhibited using EPON 934 adhesive. The Pyro-Pak assembly is made from a stafoam spacer with two pockets cut in it, into which 0.1 gm of BKNO_3 is loaded into the pockets and retained by onion-skin paper bonded to both sides with EPON 934. The pyrogen chamber is spot-sanded on all bonding surfaces and washed with methyl ethyl ketone. The SCID is positioned in the chamber and bonded in place using EPON 934. The SCID is then bent into position with specialized tooling, and the Pyro-Pak is positioned in the chamber using an interference fit to hold it in position while the adhesive is curing (EPON 934). The plug/grain assembly and the SCID/chamber/Pyro-Pak assembly are mated with an O-ring, which is lubricated and slipped in place on the pyrogen plug. The chamber then is pressed down over the plug and secured in place with roll pins. Assemblies are then packaged awaiting final assembly of motor.

Thrust Chamber/Spin Motor Assembly

The igniter assembly is inserted into the loaded thrust chamber through the igniter boss with an O-ring in place;

Fig. 2 Exploded view of motor.



it is held in position with a snap ring. PR-1221-B2 sealant is applied between the chamber threads and the aft face of propellant grain. Loctite is applied to the threads of the chamber and the spin motor/aft closure assembly is threaded over the main motor SCID lines and installed into the exit cone using PR-1221-B2 sealant. The aft end of the closure is sealed with PR-1221-B2 sealant and cured for 2 hr at 120°F.

Spin-motor nozzle plugs are positioned and bonded on the spin motor ignition harness using PR-1221-B2 and cured for 2 hr at 120°F. Two of these assemblies are then bonded into the spin-motor nozzle with one solid plug using PR-1221-B2 and cured for 2 hr at 120°F. The loaded thrust chambers are sealed and stored until needed.

The ends of the SCID lines are bonded into the squib holder using EPON 934 and cured for 2 hr at 140°F. The yoke assembly is positioned on the motor, and the squib holder is positioned into the yoke assembly. The squib holder is held in place with three set screws. The spin motor SCID is positioned over the yoke release pin and held in place with a steel clip and a set screw; PR-1221-B2 then is placed around the SCID on the outside of the clip. The assembly is placed in cure for 2 hr at 120°F. An O-ring is lubricated and installed in the squib holder, and the squib holder closure is installed and secured by the collar. Any scratches on the anodized motor components are repaired by an alodine brush-on solution.

Decal and identification (Human Engineering) tags are applied to the motors. Motors are placed in special polyethylene shipping containers, and inspected, and the containers are sealed.

Concluding Remarks

This design concept provides considerable flexibility. By increasing or decreasing the spin motor propellant loading, or the burning surface of the propellant web and/or nozzle diameter, and/or the effective flow angle of the nozzle, this multipurpose motor can be quickly and easily tailored to many variable axial and tangential thrust combinations.

Lunar Mascon Effects on Orbits of Apollo-Type Spacecraft

IRVING MICHELSON*

Illinois Institute of Technology, Chicago, Ill.

Introduction

SINCE the discovery of large concentrations of mass under certain areas of the moon's surface in August 1968, their influence in modifying the trajectories of lunar orbiters has been verified by Apollo 8 and by Apollo 10 spacecraft. The mascons, as they have become known, present real hazards to navigation as long as they remain less than fully identified. Detailed measurements and calculations may not be completed for a year or more, but preliminary calculations like the one described herein can provide a useful practical guide for minimizing mascon-induced orbital instabilities. Specifically, it is shown that the judicious selection of orbital apse direction is particularly effective for this purpose.

Characteristics of Mass Concentrations in the Moon

Careful analysis of Lunar Orbiter satellite tracking data¹ led to the conclusion that unpredicted orbital changes were

caused by enormous mass concentrations apparently situated beneath the surface of five near-side maria. The mascon under Mare Imbrium is estimated to be upwards of 100 miles in diameter and to represent about 1/200,000 of the total mass of the moon; the group of mascons may total 1/50,000 of the moon's mass. Subsequently their presence was confirmed when Apollo 8 orbit exhibited pronounced and unpredicted variations. Specifically, the apolune distance (maximum orbital distance from the lunar centroid) increased measurably from one circuit to the next in a manner the exact opposite of the familiar orbital decay of Earth satellites. In the latter case atmospheric resistance to spacecraft motion leads to decreasing apogee distance. Since the moon lacks an atmosphere but possesses mascons instead, the supposition was made that the mascons are responsible for the anomalies of the Apollo 8 orbit and those of the more recent Apollo 10. Precise knowledge of mascon locations and magnitudes, required for calculating trajectory corrections for Apollo 11 and other close lunar orbiters is not presently available but awaits further progress in lunar studies.

Simplified Estimation of Mascon Orbital Influence

In the absence of accurate data on the mascon sizes and positions that determine the appropriate perturbation Hamiltonian functions for precise computation, a useful first estimate of the orbital modifications they produce is accomplished by elementary methods. By regarding the orbit as a Keplerian ellipse, the perilune distance r_1 is expressed in terms of the standard parameters semi-major axis a and eccentricity e by the formula

$$r_1 = a(1 - e)$$

When it is recalled that in a reference frame moving with the moon, the rotation of which is ignored, the mascons are stationary and therefore do not modify the energy of motion of spacecraft during a near-passage encounter, it follows that a remains constant but not necessarily the eccentricity e . Perilune modification in one orbital cycle is denoted δr_1 and consequently related to the modified eccentricity δe by the formula

$$\delta r_1 = -a\delta e \quad (1)$$

It is clear that perilune change δr_1 depends on how the eccentricity of the orbit is altered by the encounter with the mascons, and the same is true of the apolune distance r_2 given by $a(1 + e)$. D'Alembert's classic technique for studying the motion of Lexell's comet of 1770 may be adapted to treat the flyby of Apollo 11 in the vicinity of the mascons in a manner reminiscent of the comet's flyby encounter with the planet Jupiter. Specifically, the fact that the duration of the appreciable attraction by the mascons is small compared to the orbital period suggests idealizing the encounter as instantaneous (the same idea is employed in approximate analysis of rocket vehicle performance, the thrust being treated as impulsive). Then the orbit of the spacecraft is made up of elliptic segments connected by a certain discontinuity that represents the total effect of the flyby encounter.

The (discontinuous) change δe is then expressed in terms of the corresponding change of the areal constant h (given by the square root of $\mu a(1 - e^2)$ where μ is the moon's gravitational constant proportional to its mass M);

$$\delta h/h = -e\delta e/(1 - e^2) \quad (2)$$

The areal constant h is also expressible in terms of the orbital distance r , orbital speed q , and the path angle γ defined as the complement of the angle formed by extending the radial line from the moon to the spacecraft, and the direction of the velocity vector corresponding to q . The relationship is simply

$$h = rq \cos \gamma$$

Received June 3, 1969; revision received September 8, 1969. Helpful discussion with H. Buning is gratefully acknowledged.

* Professor of Aerospace Engineering. Member AIAA.